Ottawa, Canada
ACTIVE 2009
2009 August 20-22

Combined MIMO adaptive and decentralized controllers for broadband active noise and vibration control

A. P. Berkhoff*† [a], J. M. Wesselink†

*TNO Science and Industry, MON-Acoustics
PO Box 155, 2600AD Delft, The Netherlands

†University of Twente, EEMCS-Signals and Systems
PO Box 217, 7500AE Enschede, The Netherlands

ABSTRACT

Recent implementations of multiple-input multiple-output adaptive controllers for reduction of broadband noise and vibrations provide considerably improved performance over traditional adaptive algorithms. The most significant performance improvements are in terms of speed of convergence, the amount of reduction, and stability of the algorithm. Nevertheless, if the error in the model of the relevant transfer functions becomes too large then the system may become unstable or lose performance. On-line adaptation of the model is possible in principle but, for rapid changes in the model, necessitates a large amount of additional noise to be injected in the system. It has been known for decades that a combination of high-authority control (HAC) and low-authority control (LAC) could lead to improvements with respect to parametric uncertainties and unmodeled dynamics. In this paper a full digital implementation of such a control system is presented in which the HAC (adaptive MIMO control) is implemented on a CPU and in which the LAC (decentralized control) is implemented on a high-speed Field Programmable Gate Array. Experimental results are given in which it is demonstrated that the HAC/LAC combination leads to performance advantages in terms of stabilization under parametric uncertainties and reduction of the error signal.

1 INTRODUCTION

Many algorithms used for broadband active noise control are based on the adaptive Least-Mean-Square (LMS) algorithm [1]. The low complexity and the relatively good robustness properties are the major advantages of the LMS algorithm. Recent algorithms solve many of the problems associated with the speed of convergence of the older algorithms. One such algorithm, which is based on the filtered-error algorithm because the latter algorithm is more efficient for multiple reference signals than the filtered-reference algorithm, is the regularized modified filtered-error algorithm. This algorithm uses the inverse of the minimum-phase factor of the secondary path, combined with a double set of control filters to eliminate the negative effect of the delay in the adaptation loop [2]. The latter algorithm is combined with a regularization technique that preserves the factorization properties [2]. Extensions were given for colored reference signals [3], which also potentialy lead to reduced convergence rates. The regularized modified filtered-error least mean square algorithm (RMFeLMS) has good robustness and convergence properties as compared to the filtered-reference and filterer-error algorithm. However, the controller is model-based and is therefore still sensitive for mismatch between the model and the plant. This model mismatch reduces the overall performance of the controller. Model mismatch can be caused by variations in parameters such as temperature, boundary conditions etc. On-line adaptation of the model is possible in principle but necessitates a large

[a] Email address: arthur.berkhoff@tno.nl, a.p.berkhoff@utwente.nl

amount of additional noise to be injected in the system for rapid changes in the model [4]. An alternative approach is to use a high-authority and low-authority control (HAC/LAC) architecture [5] where the goal of the low-authority controller is to add active damping to the structure. Active damping can be implemented using different strategies. The use of a HAC/LAC architecture yields three major advantages [5]. Firstly, the active damping extends outside the bandwidth of the HAC control loop, which reduces the settling times outside the control bandwidth. Secondly, it is easier to gain-stabilize the modes outside the bandwidth of the outer loop. And thirdly, the large damping of the modes inside the controller bandwidth makes them more robust to parametric uncertainty. In the paper by Herold et al. [6], a method using piezoelectric sensors and actuators and positive position feedback (PPF) was described. In the PPF-method, a second-order filter is used as the control filter which is combined with positive feedback. The control filter is then tuned to reduce one of the desired resonance peaks.

In the present paper, an approximately collocated and dual sensor-actuator pair is used, suitable for broadband damping as described by Elliott et al. [7]. If the actuator-sensor system is dual and collocated, a simple decentralized proportional feedback controller is sufficient to add damping due to the fact that the overall energy that is stored in the system will be reduced [5]. Active damping is not very effective for frequencies that do not coincide with the poles and zeros. To gain further reductions for such frequency components a model-based controller is used such as the RMFeLMS algorithm as described in this paper. A relatively high sample rate is used for decentralized control whereas a lower sample rate is used for centralized control, such as for the HAC/LAC methodology. The LAC algorithms, which are relatively simple but run at high sample rates were realized efficiently on reconfigurable hardware, such as an FPGA. The HAC algorithms, which are relatively complex and which run at relatively low sample rates, were realized on a general purpose Central Processing Unit (CPU).

2 METHODS

The HAC/LAC architecture was tested on a piezoelectric panel for reduction of noise transmission, a cross-section of which can be found in Fig. 1. Five piezoelectric patch actuators and five piezoelectric patch sensors were attached to the panel [3]. The panel was built from two Printed Circuit Boards (PCBs) with a honeycomb layer in between. One advantage of this approach is that electronics can be integrated. Another advantage is that the actuator and the sensor can be placed on different faces of the panel, which improves the control of the acoustically relevant out-of-plane vibrations because the in-plane coupling between the actuator and the sensor is reduced [8]. In addition, five collocated accelerometers were used for active damping with decentralized control using the piezoelectric patch actuators.

In many publications, active damping is realized using an analog controller [9;10;11]. One of the advantages of an analog controller is its low delay when compared to a digital controller. In this paper, a method is described that uses a digital controller with a high-sample rate that approximates an analog controller, such that the analog and digital controllers have identical performance for frequencies within the control bandwidth. The existing control architecture provided a suitable environment for realization of such a high speed digital feedback controller. The analog interface board already contained ADDA converters operating at a sample rate of 100 kHz while the actual RMFeLMS algorithm was operating at a lower sample rate, in this case 2 kHz. This made it possible to run the LAC and HAC controller at different sample rates. The interface between the PCI-104 system running the HAC algorithm and the ADDA unit was implemented in reconfigurable hardware, in this case a Field Programmable Gate Array (FPGA),(See Fig. 2). The FPGA incorporates the

following functional units: the decimation filters, the interpolation filters, the glue logic for the PCI bus interface and the low-authority controller. The decimation filters and interpolation filters were designed in such a way that the desired compromise between group-delay and stopband attenuation was obtained. This same architecture was realized as a distributed system, where spatially distributed high-speed controllers were acting locally, whereas control at low to medium sample rates was performed globally[12]. In such a configuration, all the local, decentralized FPGA-based controllers are connected to the central controller by means of a network. This network has low latency, low jitter, guaranteed response times and allows feedback control[13] at frequencies up to approximately 10 kHz over the network. However, for the experiments as described in the present paper all decentralized controllers were realized in a single FPGA.

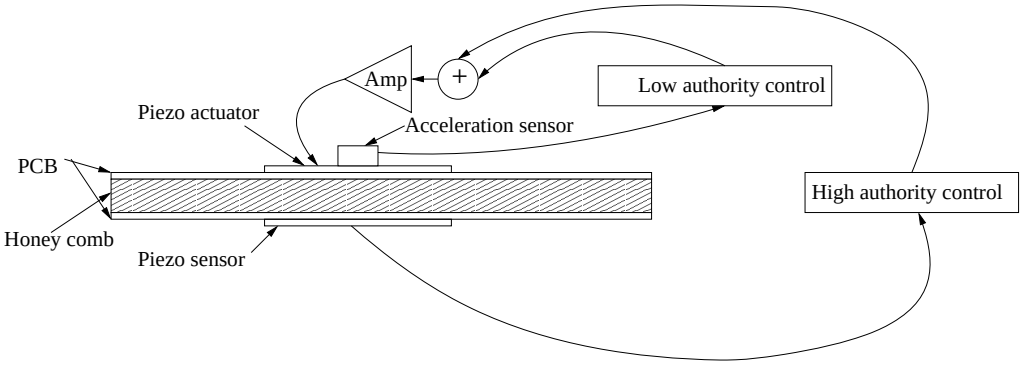

Figure 1: Configuration of the high-authority/low-authority control architecture applied to a sandwich panel with piezoelectric patch actuators, piezoelectric patch sensors and accelerometers.

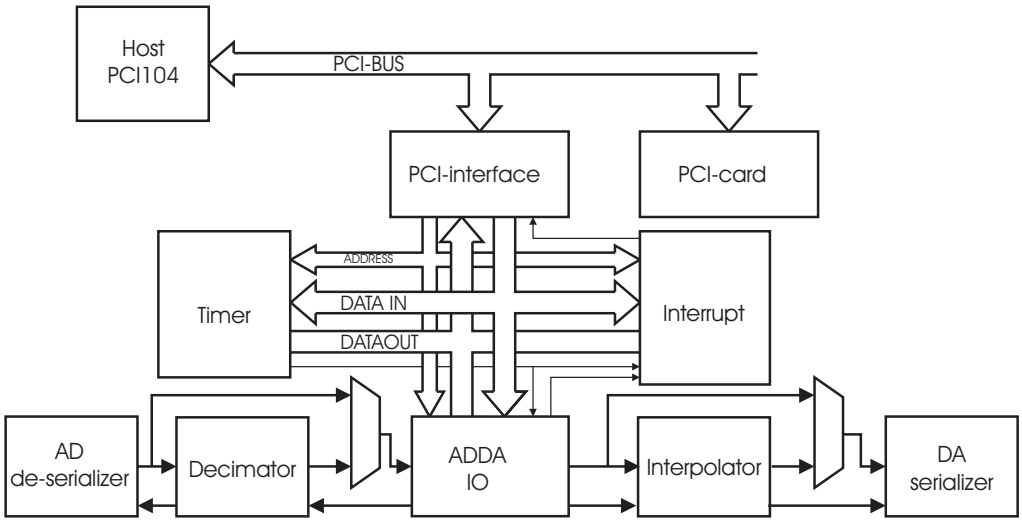

Figure 2: Architecture of the FPGA without LAC-unit.

A block diagram of the multiple-input multiple-output adaptive controller as used for the high-authority controller is shown in Fig. 4. A detailed description of this algorithm can be found in Refs. 2, 3. Relevant for the experiments as described in this paper are the definition of the update rule for the controller and the regularization of the secondary path. For the description of the MIMO controller, we assume that there are K reference signals, L error sensors and M actuators. Denoting

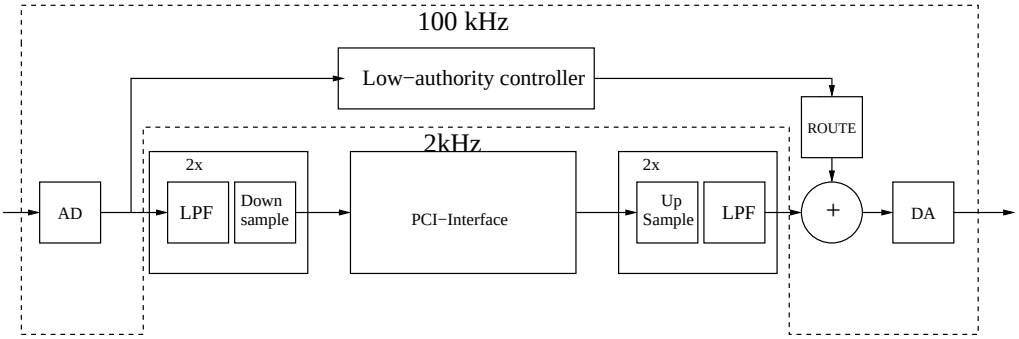

Figure 3: Simplified block diagram of the control system containing the low-authority controller.

n as the sample instant, the update rule for the controller coefficients is

$$W_i(n+1) = W_i(n) - \alpha e''(n) x'^T(n-i), \tag{1}$$

in which the i-th filter coefficients of the control filters are represented by the $M \times K$ matrix W_i, where $i = 0..I-1$, i.e., $W(q) = \sum_{i=0}^{I-1} q^{-i} W_i$, with q the unit delay operator. Furthermore, $e''(n)$ is the $M \times 1$ vector of auxiliary error signals, $x'(n)$ is the $K \times 1$ vector of delayed reference signals, and α is the convergence coefficient.

The regularization was implemented by defining an augmented plant $\overline{G}(q)$:

$$\overline{G}(q) = \begin{bmatrix} G(q) \\ G_{\text{reg}}(q) \end{bmatrix}, \tag{2}$$

in which the $L \times M$-dimensional secondary path $G(q)$ is augmented with an $M \times M$-dimensional transfer function $G_{\text{reg}}(q)$. For the implementation as described in this paper, the regularization was based on a simple weighting of the $M \times 1$ vector of control signals $u(n)$, which also limits the amplification of near-zeros of $G(q)$ in the $M \times M$-dimensional inverse $\overline{G}_o(q)^{-1}$. For this purpose, the regularizing transfer function $G_{\text{reg}}(q)$ was defined as:

$$G_{\text{reg}}(q) = \sqrt{\beta} I_M, \tag{3}$$

in which β is a scalar quantity and in which I_M is an $M \times M$ identity matrix.

3 RESULTS

For the idealized low-authority controller having the purpose to add damping to the system the phase should be between -90 and +90 degrees for each collocated pair. Figs. 5 and 6 can be used to judge the practical setup involving the piezoelectric patch actuator and the accelerometer regarding this requirement. In Fig. 5, it can be seen that for frequencies up to 1 kHz the phase is between -90 degrees and +90 degrees. In Fig. 6, however, it can be seen that for higher frequencies the phase lag is larger. Based on these results, the decentralized controllers were configured with a 1st-order roll-off above 1 kHz. The influence of the local controllers on the measured transfer function of the high-authority controller is shown in Fig. 7. It can be seen that resonances and antiresonances can be damped, particularly at low frequencies. For higher frequencies and for higher feedback gains some spillover can be observed. For this particular configuration also a controller configuration was tested in which the center actuator-sensor pair had a higher gain than the other pairs (see Fig. 7). Of

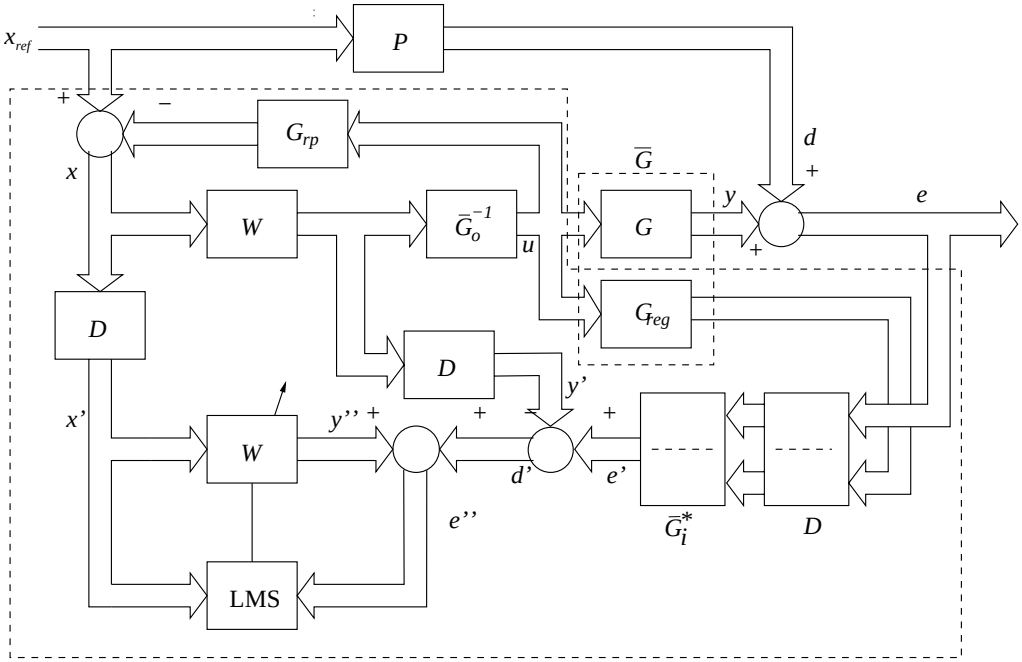

Figure 4: Regularized modified filtered-error adaptive control scheme with IMC[2;3].

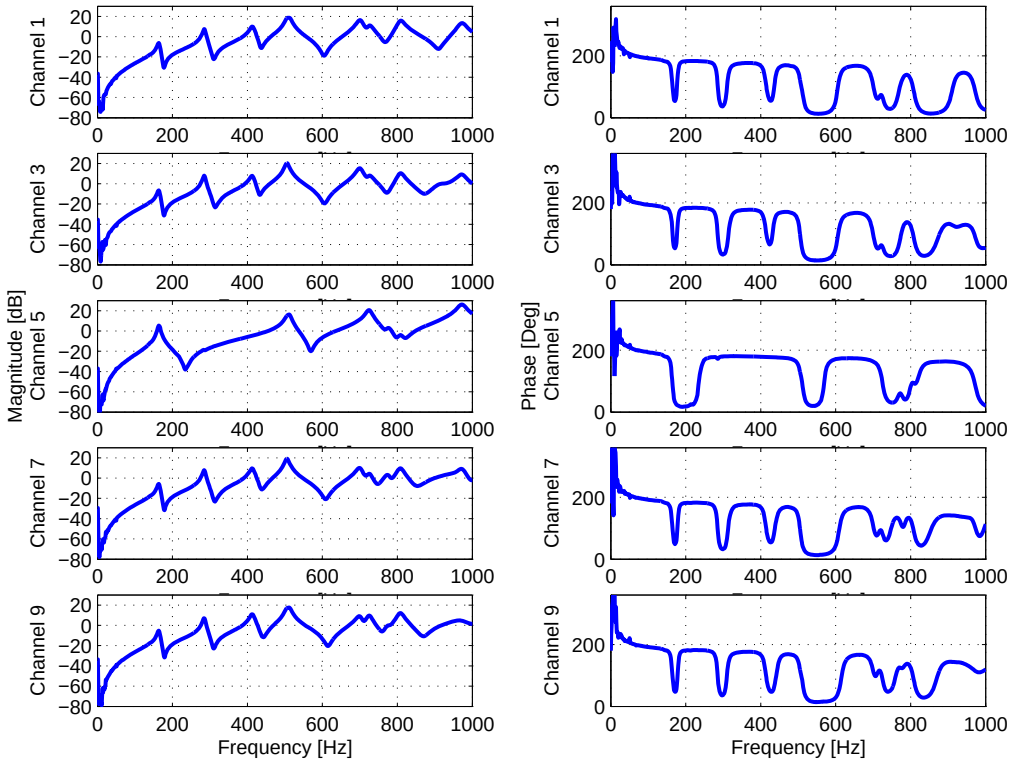

Figure 5: The transfer functions for the collocated sensor-actuator pairs from 0 to 1 kHz; piezoelectric actuator to acceleration sensor, 5 pairs of the available 9 pairs were used.

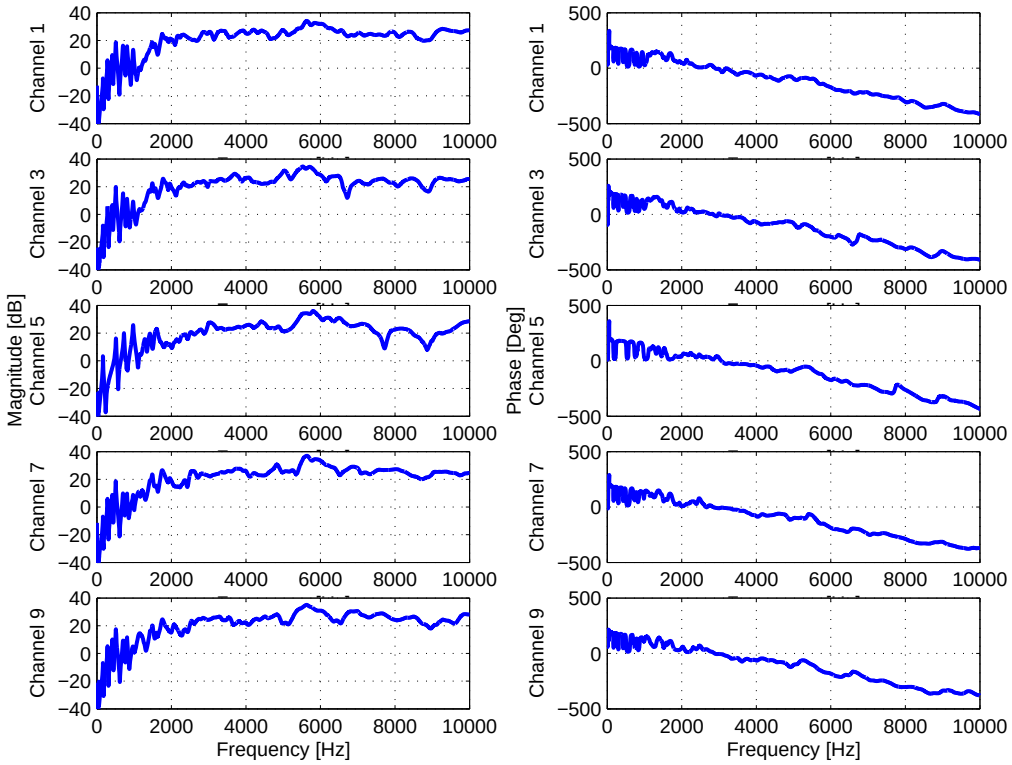

Figure 6: As Fig. 5, except that the frequency range is 0 - 10 kHz.

the configurations studied, this configuration was found to be a good compromise between damping performance and spillover.

Control results for a HAC/LAC architecture using an adaptive MIMO *feedback* algorithm are shown in Fig. 8. For this result, the regularization parameter β was set to -20 dB. The convergence coefficient was set to $\alpha = \frac{1}{80}$, which was the value that resulted in the highest reduction at 60 seconds after start of the convergence. It can be seen that the reduction of the error signals for MIMO control (HAC) is higher than for the decentralized control (LAC). However, the combination of HAC and LAC leads to the largest reduction of the error signals. The average improvement by adding the low-authority controller to the high-authority controller is approximately 1.4 dB.

Control results for a HAC/LAC architecture using an adaptive MIMO *feedforward* algorithm are shown in Fig. 9. For this result, the regularization parameter β was set to -30 dB, and the convergence coefficent to $\alpha = \frac{1}{40}$, which was the value that resulted in the highest reduction at 60 seconds after start of the convergence. It can be seen that the reduction of the error signals for MIMO control (HAC) is considerably higher than for the decentralized control (LAC). However, as with feedback control the combination of HAC and LAC leads to the largest reduction of the error signals. The average improvement by adding the low-authority controller to the high-authority controller is approximately 4.4 dB.

A subsequent set of tests was performed to study the influence of LAC on the robustness of the controller. The robustness was evaluated by adding different weights to the piezoelectric panel. The high-authority controller for these tests was based on a model that was obtained without the additional weight. Fig. 10 shows the phase difference between the situations with added mass and without added mass of the models as identified for the high-authority controller for the cases that the low-authority controller was switched on and for the case that the low-authoriy controller was

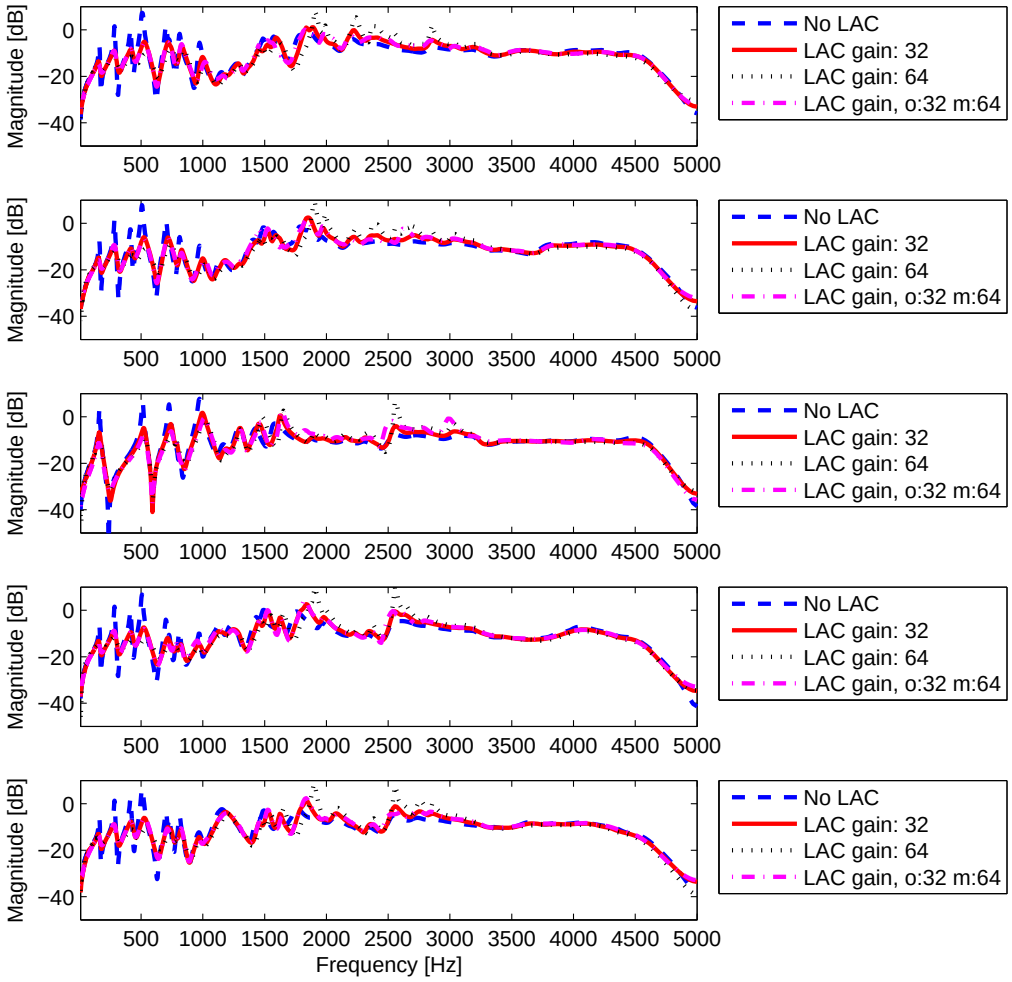

Figure 7: Influence of low-authority controller on the transfer function of the plant, as measured from the piezoelectric actuator to the piezoelectric sensor, while the feedback loop was from the actuator to the acceleration sensor. The decimation filter was switched off; an interpolation filter with a stopband attenuation of 50 dB was used.

switched off. In this figure, it can be seen that for low frequencies the system is less sensitive to the addition of mass when the low-authority controller is switched on. Therefore it was expected that the robustness of the present high-authority controller would benefit from the addition of the low-authority controller since the robustness of the adaptive high-authority controller is primarily determined by the phase of the secondary path [14].

Indeed, the robustness of the adaptive controllers improved by the addition of the low-authority controller. The results for the robustness of the adaptive feedback controller are summarized in Table 1. This table contains the average reductions of the error signals provided the system was stable. The reductions are given for different values of added weight as well as different values of the regularization of the controller. It can be seen from the results in this table that, firstly, larger weights can be added if LAC is switched on, and therefore the robustness improves by the addition of LAC, secondly, that higher levels of the regularization parameter β also lead to increased robustness, and thirdly, for low values of β the improvement by LAC is marginal. Furthermore, the regularization by β does not seem to influence the robustness if LAC is switched off. Especially for regularization

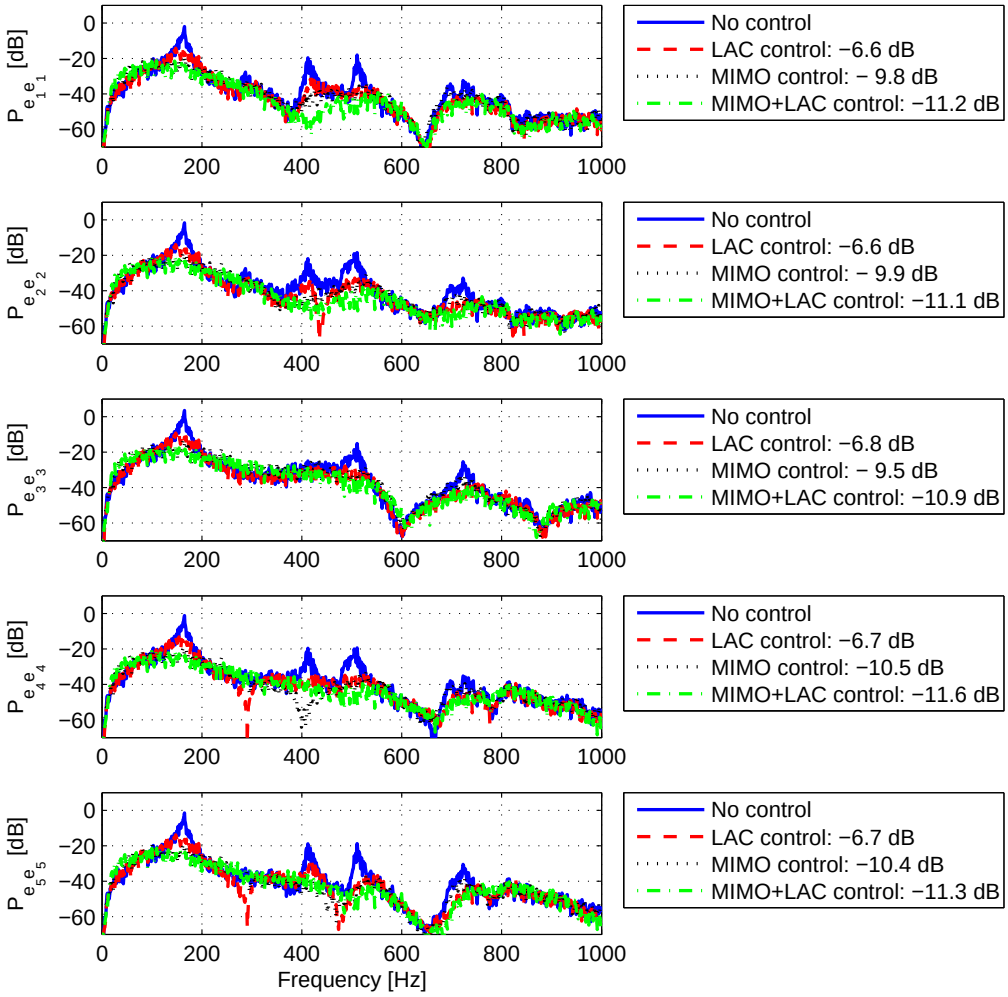

Figure 8: Performance measured on the sensors for a feedback controller using IMC.

levels of β=-20 dB and β=-25 dB there is a significant improvement of the robustness by the addition of LAC. Similar results can be found for the feedforward controller, as shown in Table 2, although in this case the emphasis of the improvement is on the reduction of the mean square value of the error signal instead of the robustness. The relative importance of the robustness and the reduction of the mean-square error is influenced by the value of the regularization level β, which was not equal for the feedforward controller and the feedback controller. The regularization level for the feedback controller was set to a somewhat higher level than for the feedforward controller. One reason is that, on the one-hand, it doesn't make sense to use an extremely small regularization level for feedback controllers since it will not reduce the mean-square error anymore. On the other hand, if the value of the regularization level is set too high for a feedforward controller then the performance gain of a feedforward controller over a feedback controller is relatively small.

An interesting observation was that the robustness of the adaptive feedback controler also increased if the model was obtained with LAC switched on but for which, during control operation, the LAC was switched off. The results of these tests can be found in Table 3. Apparently, the reduced phase in the model itself is beneficial for the robustness of the controller.

Table 1: Influence of added weight on the performance of a feedback controller. The reduction was measured after 180 seconds and was the average MSE over all 5 sensors. A step size $\alpha = \frac{1}{40}$ was used. The model for IMC and the RMFeLMS algorithm were identified without the additional weight.

Weight	β = -20 dB		β = -25 dB		β = -30 dB	
[gram]	LAC [dB]	LAC off [dB]	LAC [dB]	LAC off [dB]	LAC [dB]	LAC off [dB]
00.00	11.42	10.42	11.98	10.50	12.11	11.77
18.17	11.45	10.39	12.36	10.94	13.01	11.63
27.00	11.55	10.32	12.54	10.95	12.38	11.29
33.82	11.56	10.35	12.66	11.22	12.82	11.59
40.60	12.19	-	11.83	-	12.81	-
47.32	11.50	-	11.76	-	-	-
54.17	12.18	-	12.43	-	-	-
61.05	11.51	-	12.34	-	-	-
67.85	12.03	-	12.71	-	-	-
74.96	11.87	-	12.02	-	-	-
81.67	11.83	-	12.21	-	-	-
88.41	11.67	-	12.62	-	-	-
95.22	11.89	-	-	-	-	-

Table 2: Influence of weight on the performance of a feedforward controller. The performance was measured after 180 seconds. A step size $\alpha = \frac{1}{40}$ was used. The model for the RMFeLMS algorithm was identified without additional weight.

Weight	β = -25 dB		β = -30 dB		β = -35 dB	
[gram]	LAC [dB]	LAC off [dB]	LAC [dB]	LAC off [dB]	LAC [dB]	LAC off [dB]
00.00	25.42	21.35	27.53	22.17	27.62	22.57
18.17	25.27	21.59	26.94	21.51	28.68	22.83
27.00	24.70	-	26.24	-	27.33	-
33.82	25.21	-	22.61	-	-	-
40.60	-	-	-	-	-	-

Table 3: Influence of added weight on the performance of a feedback controller. The performance was measured after 180 seconds. A step size $\alpha = \frac{1}{40}$ was used. In this case the LAC unit was switched off but the model used LAC and was used for IMC and the RMFeLMS controller. This model was identified without additional weight but with LAC switched on. The regularization level β was set to -25 dB.

Weight [gram]	00.00	18.17	27.00	33.82	40.60	47.32	54.17	61.05	67.85
Reduction [dB]	11.25	11.73	11.94	11.63	11.74	11.35	11.36	11.45	-

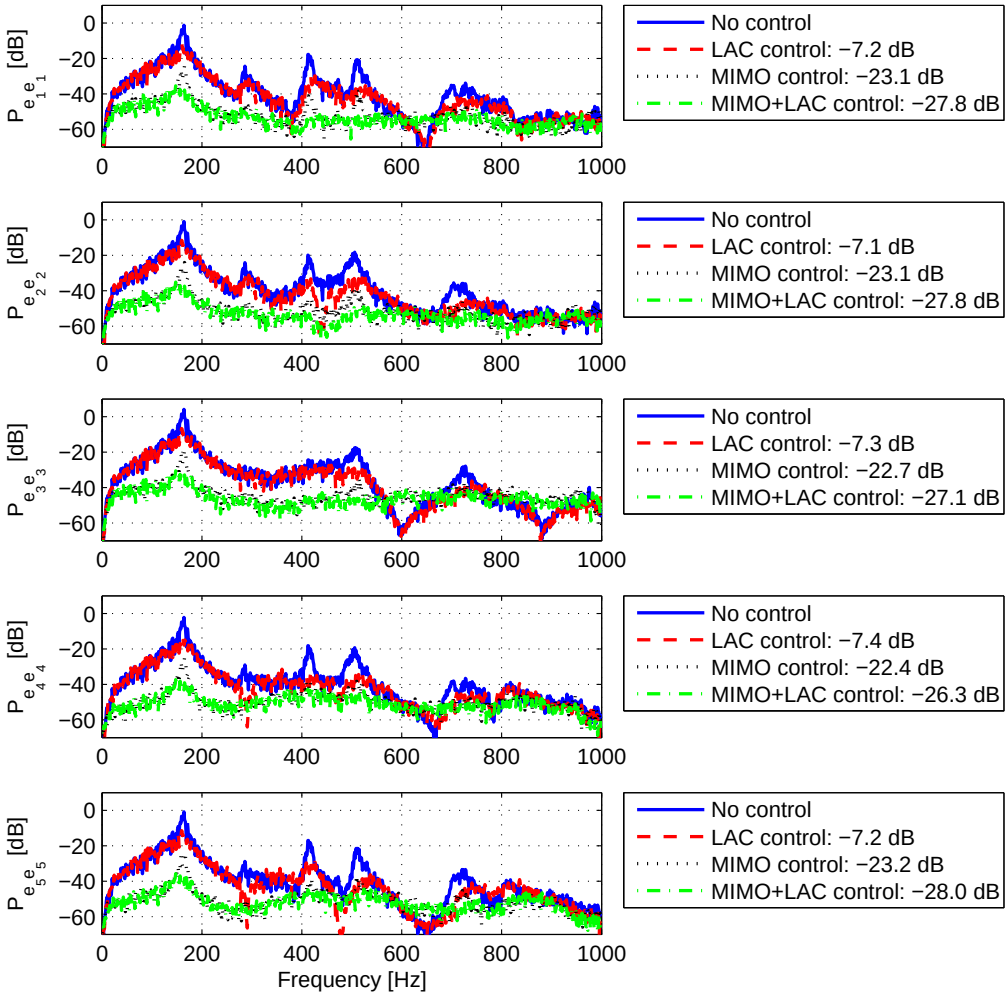

Figure 9: Performance of the feedforward controller.

4 CONCLUSION

In this paper it was shown that recent advances in signal processing and integrated circuit design make it possible to implement a full digital HAC/LAC architecture operating at relatively high sample rates as required for active noise reduction. The HAC/LAC architecture was realized as a high-speed decentralized controller on FPGA and a medium speed centralized controller on a CPU. For the configurations that were studied, the increase in robustness was most noticeable for an adaptive feedback controller, whereas, for the adaptive feedforward controller, the improvement of performance was most noticeable with respect to the reduction of the mean-square value of the error signals.

5 ACKNOWLEDGEMENTS

The authors would like to thank Geert Jan Laanstra and Henny Kuipers of University of Twente, Signals and Systems group, Faculty EEMCS for the excellent support.

REFERENCES

[1] S. M. Kuo and R. D. Morgan, *Active Noise Control Systems* (John Wiley & Sons, Inc, United States of America) (1996).

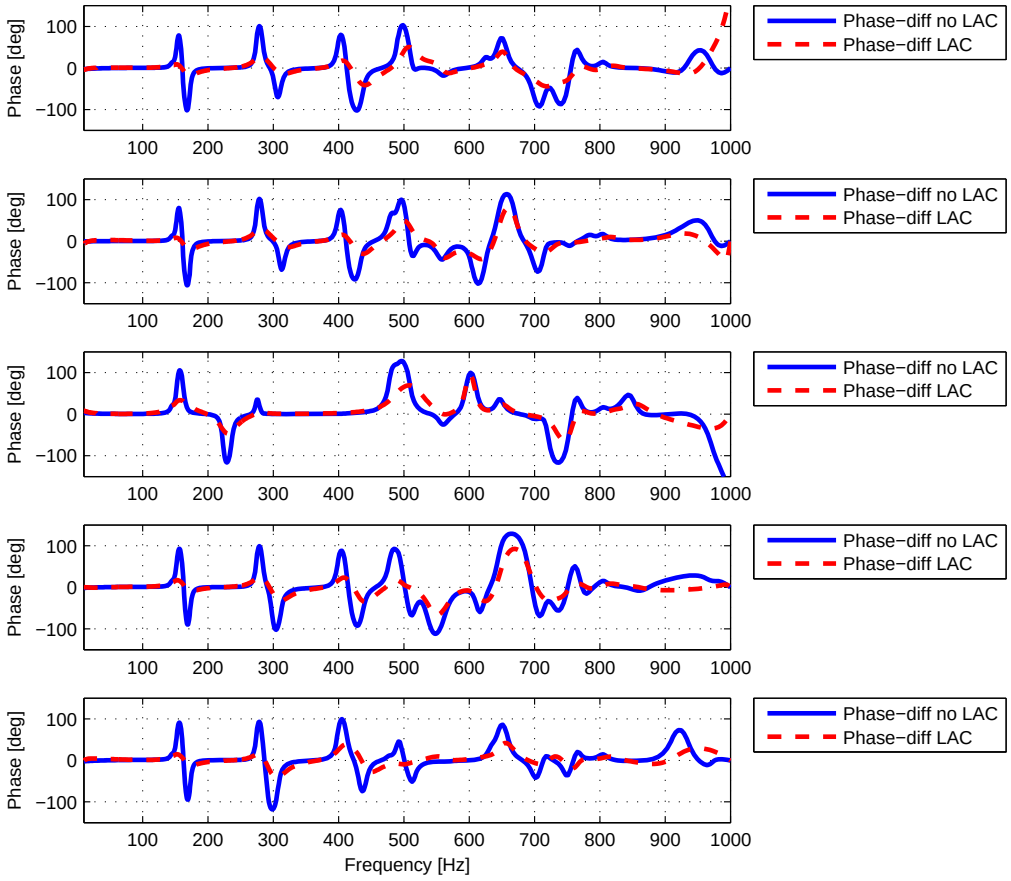

Figure 10: A plot of the difference in phase between systems with and without additional weight. The first curve uses no LAC and the second one has LAC enabled. In this case a weight of 40.60 gram was added to the panel.

[2] A. P. Berkhoff and G. Nijsse, "A rapidly converging filtered-error algorithm for multichannel active noise control", International Journal of Adaptive Control and Signal Processing **21**, 556–569 (2007).

[3] J. M. Wesselink and A. P. Berkhoff, "Fast affine projections and the regularized modified filtered-error algorithm in multichannel active noise control", The Journal of the Acoustical Society of America **124**, 949–960 (2008).

[4] S. Elliott, *Active Sound and Vibration Control*, chapter 3, Adaptive methods in active control, 57–72 (IET, Londen) (2002).

[5] A. Preumont, *Vibration Control of Active Structures*, 2nd edition (Kluwer Academic Publishers, Dordrecht) (2002).

[6] S. Herold, D. Mayer, and H. Hanselka, "Transient simulation of adaptive structures", Journal of Intelligent Material Systems and Structures **15**, 215–224 (2004).

[7] S. J. Elliott, P. Gardonio, T. C. Sors, and M. J. Brennan, "Active vibroacoustic control with multiple local feedback loops", J Acoust Soc Am **111**, 908–915 (2002).

[8] A. P. Berkhoff, "Weight reduction and transmission loss tradeoffs for active/passive panels with miniaturized electronics", in *Proc. Active 04*, edited by R. H. Cabell and G. C. Maling, 1–12 (INCE USA, Washington DC) (2004).

[9] P. Gardonio, E. Bianchi, and S. J. Elliott, “Smart panel with multiple decentralized units for the control of sound transmission. part i: theoretical predictions”, Journal of Sound and Vibration **274**, 163–192 (2004).

[10] P. Gardonio, E. Bianchi, and S. J. Elliott, “Smart panel with multiple decentralized units for the control of sound transmission. part ii: design of the decentralized control units”, Journal of Sound and Vibration **274**, 193–213 (2004).

[11] E. Bianchi, P. Gardonio, and S. J. Elliott, “Smart panel with multiple decentralized units for the control of sound transmission. part iii: control system implementation”, Journal of Sound and Vibration **274**, 215–232 (2004).

[12] A. P. Berkhoff and J. M. Wesselink, “Centralised and decentralised configurations for panels with piezoelectric actuators”, in *Proceedings of Euronoise 2006*, 429 (European Acoustics Association, Tampere, Finland) (2006).

[13] J. M. Wesselink, A. P. Berkhoff, G. J. Laanstra, and H. Kuipers, “Implementation issues of a high-speed distributed multi-channel adda system”, in *International Workshop on Acoustic Echo and Noise Control IWAENC* (IWAENC, Eindhoven) (2005).

[14] S. J. Elliott, *Signal Processing for Active Control* (Academic Press, Harcourt Place, 32 Jamestown Road, London NW1 7BY, UK) (2001).